

Power Spectrum Analysis of an Anthropomorphic Breast Phantom Compared to Patient Data in 2D Digital Mammography and Breast Tomosynthesis

Lesley Cockmartin^{1,*}, Predrag R. Bakic², Hilde Bosmans¹, Andrew D.A. Maidment², Hunter Gall³, Moustafa Zerhouni³, and Nicholas W. Marshall¹

¹ KU Leuven, Department of Imaging and Pathology, Division of Medical Physics and Quality Assessment, Herestraat 49, 3000 Leuven, Belgium

² University of Pennsylvania, Department of Radiology, 1 Silverstein Building HUP, 3400 Spruce Street, Philadelphia, PA 19104-4206

³ Computerized Imaging Reference Systems (CIRS), Inc., 2428 Alameda Ave, Suite 316 Norfolk, Virginia 23513 USA

{Lesley.Cockmartin, Hilde.Bosmans, Nicholas.Marshall}@uzleuven.be,
{Predrag.Bakic, Andrew.Maidment}@uphs.upenn.edu,
{hgall, zerhounim}@cirsinc.com

Abstract. Digital breast tomosynthesis (DBT) images of a novel anthropomorphic breast phantom (UPenn phantom) acquired on two breast tomosynthesis systems were analyzed in terms of their power spectra (PS). The β and κ power law coefficients were estimated from 2D planar, tomosynthesis projection images and reconstructed planes. These data were compared to the PS characteristics as retrieved from a group of patient data. Power spectra of the UPenn phantom images were very similar to the patient data, with power law parameters in the range of values found in patients. Power law exponents were 2.99 and 3.45 for 2D, 2.87 and 2.75 for DBT projections and, 1.92 and 3.10 for DBT reconstructions for the Siemens and Hologic system respectively. The agreement was better than with other (non-anthropomorphic) 3D structured phantoms, making this phantom a good candidate test object for DBT performance testing.

Keywords: digital breast tomosynthesis, digital mammography, phantom, breast structure, power spectrum analysis.

1 Introduction

Digital breast tomosynthesis (DBT) acquires a series of projections of the breast from which a stack of slices is reconstructed. DBT should improve the detection and characterization of breast lesions based on two main features: (1) lesions show up in one or a few planes, providing depth information; (2) the tissue superposition from breast structures at a distance from the plane of interest is reduced, improving the detectability and

* Corresponding author.

delineation of the lesions. In order to compare existing breast imaging modalities to DBT, these aspects have to be taken into consideration. Proper performance testing should define a task and an associated figure of merit. In the case of comparative studies between 2D mammography and DBT, the detection of a 3D lesion in a structured background would be a good candidate performance test.

Most existing anthropomorphic test objects, developed for projection mammography, have structures in a relatively thin 3D slab. There is therefore a need for another type of phantom, preferably a 3D anthropomorphic test object. This study focuses on a newly designed breast phantom (UPenn phantom, CIRS Inc., VA, USA), which is based on a previously developed anthropomorphic software phantom [1, 2]. The UPenn phantom had been developed for the use in preclinical and clinical assessment of image quality in 2D and 3D breast imaging systems. Whereas the anatomy of the breast has been mimicked as closely as possible, it remained to be determined how this structured phantom would compare to real patient data. In this paper, planar 2D and DBT images of this phantom, acquired on two different DBT systems, were evaluated in terms of power spectrum analysis. We calculated power spectra and power law coefficients of the newly designed phantom, acquired at different dose levels in 2D and DBT mode. Then we compared the resulting power spectra to previously published power spectra of a group of patients and additionally also to the power spectra of three other phantoms developed for DBT [3]. Finally, mean glandular doses (MGD) of the phantom were compared to patient doses.

2 Methods and Materials

2.1 Anthropomorphic Phantom

The design of the physical UPenn phantom (CIRS Inc., VA, USA) was based on the previously developed anthropomorphic software UPenn phantom which contains realistically arranged anatomical structures, including skin, adipose tissue compartments, Cooper's ligaments and regions of dense fibro-glandular tissue [1, 2]. By simulating a realistic arrangement of breast tissue structures, the phantom provides an anatomically correct complex tissue background, designed for consistent validation of various breast imaging modalities. The phantom consists of precisely distributed breast equivalent materials that mimic the realistic arrangement of tissue structures, thus demonstrating in projection images how underlying targets can be masked by overlapping normal tissue structures. The complete phantom simulates a 450 ml breast with compressed thickness of 5 cm and volumetric breast density of 17% (excluding the skin). The accompanying software phantom provides detailed ground truth of the anatomy simulation, allowing for direct quantitative assessment of measurements.

2.2 Phantom Acquisitions and Patient Dataset

Patient datasets together with their power spectrum and power law parameter calculations were previously described in literature [3]. Patients had been imaged on a Siemens Inspiration (Siemens, Erlangen, Germany) and a Hologic Selenia Dimensions

system (Hologic, MA, USA) using the routine DBT settings. In total 50 lesion-free patient cases with 80 mammograms and 80 DBT image series were selected for the Siemens dataset and 26 patient cases including 48 mammograms and 48 DBT series for the Hologic system. Given that our hospital mainly performs DBT for further investigation of BIRADS 3, 4, or 5 cases, the majority of the lesion-free breasts contained dense fibroglandular structures.

The Siemens system acquires 25 projections covering an angle of 50 degrees and uses a W anode and Rh filter of 50 μm thick for both 2D and DBT acquisitions. The Hologic system is equipped with a W anode and Rh or Ag filter for 2D image acquisitions while for DBT Al filtration with a thickness of 700 μm is used. The unit acquires 15 projections over a 15 degree angular range. Both systems are using a version of filtered back projection for the reconstruction of DBT projection images and neither system uses an anti-scatter grid in DBT mode.

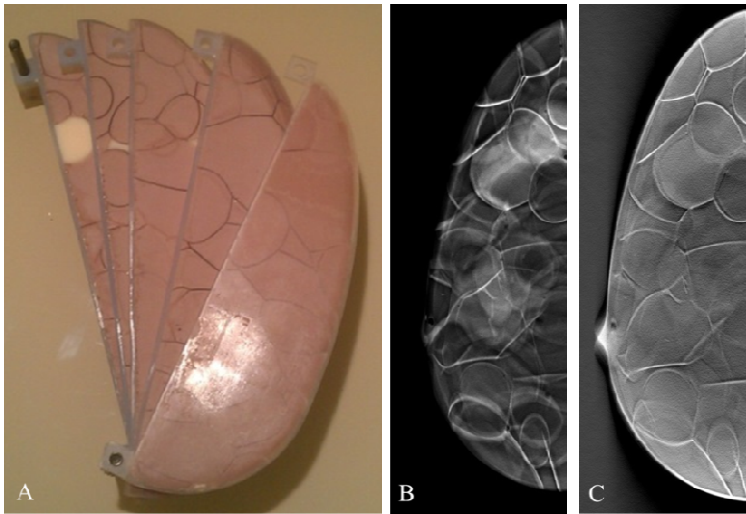


Fig. 1. Photograph of the UPenn phantom (A) and reconstructed DBT planes (B, C) acquired on the Hologic and Siemens system respectively

Table 1. Image exposure settings acquired under AEC control for the UPenn phantom, together with linearized mean PVs of the region used for the power spectrum analysis in 2D and DBT projection images. For DBT, the given tube load is the total tube load for the complete DBT acquisition.

System	Modality	Anode/filter	Tube voltage (kV)	Tube load (mAs)	PV _{linearized} ($\sim\mu\text{Gy}$)
Siemens	2D	W/Rh	29	69	70
	DBT	W/Rh	29	158	12
Hologic	2D	W/Rh	29	108	100
	DBT	W/Al	31	55	17

The UPenn phantom was imaged on a Siemens Inspiration and a Hologic Selenia Dimensions tomosynthesis system in 2D and DBT mode under automatic exposure control (AEC) (Figure 1). Automatically selected exposure settings for both modalities are tabulated in Table 1. Afterwards, a dose series was acquired by decreasing and increasing the automatically selected tube load (mAs) by 25% and 50% for both modalities.

2.3 Power Spectrum Analysis

Prior to the PS calculation, projection images were linearized using the detector response curve. Since pixel values in the reconstructed planes are largely independent of the exposure used to acquire DBT images, linearization was not possible for reconstructed images. A squared region adapted to the size of the phantom, was extracted from each projection and each reconstructed plane image in order to cover the center of the phantom. Records of size 128×128 pixels were taken from this region, half overlapping in both x and y directions. A Hanning window was applied to each record and the records were then input to a 2D PS calculation. The radial average of the 2D PS ensemble, including the 0° and 90° spatial frequency axes, was used for the power spectrum analysis. For projection images, normalization of the PS was applied by dividing by the square of the mean signal, while normalization was not applied to the PS results for the reconstructed planes. The changing in-plane pixel size of the Hologic reconstructed images was taken into account in the PS analysis. Finally, power law exponents and magnitudes, β and κ , were assessed from power law fits over the spatial frequency range of $0.2\text{--}0.7 \text{ mm}^{-1}$. Power law parameters were averaged for all 15 projection images and similarly for all reconstructed planes.

3 Results and Discussion

Table 2 gives an overview of the β and κ power law coefficients of the UPenn phantom and the range of these coefficients (mean, min, max and stdev) of the patient images for both systems. The coefficients of the UPenn phantom are within the range of those of the patients, confirming that the phantom structure consists of a similar texture as in patients. Additionally, figure 2 illustrates the PS curves of the phantom images, acquired at different dose levels and plotted against the average patient PS curve. Figure 2a shows the comparison for 2D mammographic images of the Hologic system and figure 2b for the central $\sim 0^\circ$ DBT projection images of Siemens. These graphs show that the change in dose did not influence the slope and the magnitude of the PS curve (β and κ) in the low frequency region with coefficients of variation (COV) ranging from 1% to 6% in 2D and DBT projections. This indicates that there is no influence of quantum noise within the power law region and that the PS in this region is dominated by the phantom structure. At higher frequencies, however, the quantum x-ray noise dominates and the PS curves are decreasing with increasing dose as the PS data are normalized for the signal at the detector. Figure 2 also shows the close agreement between phantom and patient PS curves, confirming the earlier agreement in power law coefficients.

Table 2. Power law exponents (β) and magnitudes (κ) for 2D, DBT projections and DBT reconstructed planes of the UPenn phantom, together with the data obtained from patient images

		2D		DBT projections		DBT reconstructed planes	
		β	κ (mm ²)	β	κ (mm ²)	β	κ (mm ²)
Siemens							
Phantom		2.99	3.21E-05	2.87	1.54E-05	1.92	1.57E+02
Patients	Mean	3.37	1.55E-05	2.92	9.02E-06	2.31	3.49E+01
	Min	2.63	5.44E-06	2.09	5.65E-06	1.39	6.39E+00
	Max	3.94	3.47E-05	3.45	1.60E-05	3.07	2.71E+02
	Stdev	0.29	5.97E-06	0.34	1.90E-06	0.38	4.77E+01
Hologic							
Phantom		3.45	2.22E-05	2.75	1.16E-05	3.10	2.23E+01
Patients	Mean	3.57	1.60E-05	2.94	4.92E-06	3.61	3.12E+01
	Min	2.81	3.28E-06	2.36	1.81E-06	2.49	1.40E+00
	Max	4.06	3.29E-05	3.71	9.55E-06	4.59	1.81E+02
	Stdev	0.26	5.91E-06	0.25	1.99E-06	0.47	3.19E+01

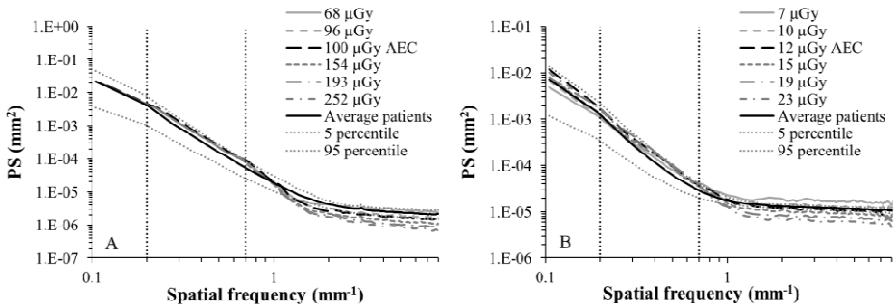


Fig. 2. Power spectrum curves of the UPenn phantom acquired at different dose levels and plotted together with the average, 5th and 95th percentile of the patient PS data for 2D mammograms of the Hologic system (A) and central DBT projection images of the Siemens system (B). The dashed vertical lines define the frequency region of the power law fit.

Next, the UPenn phantom was compared against three other structured phantoms, developed for DBT, namely the BR3D phantom (CIRS Ltd., VA, USA), the Voxmam phantom (Leeds Test Objects, UK) and the spheres in water phantom. A detailed description of these phantoms can be found in Cockmartin *et al.* [3]. The PS curve of the UPenn phantom falls within the patient PS range for both systems and both 2D and DBT images and therefore performs better than the other three structured phantoms. The PS curve of the spheres in water phantom falls within the patient range only for 2D and DBT projections of the Siemens system. The power spectrum magnitude of

the Voxmam phantom structure appears to be overall high. The BR3D CIRS phantom follows the patient curves closely in terms of power spectrum magnitude but previously reported β coefficients are generally slightly lower than the ones observed in patients [3]. Thus, the PS of the newly designed UPenn phantom has the best match to the PS of the patient data and, therefore, validates its anthropomorphic character.

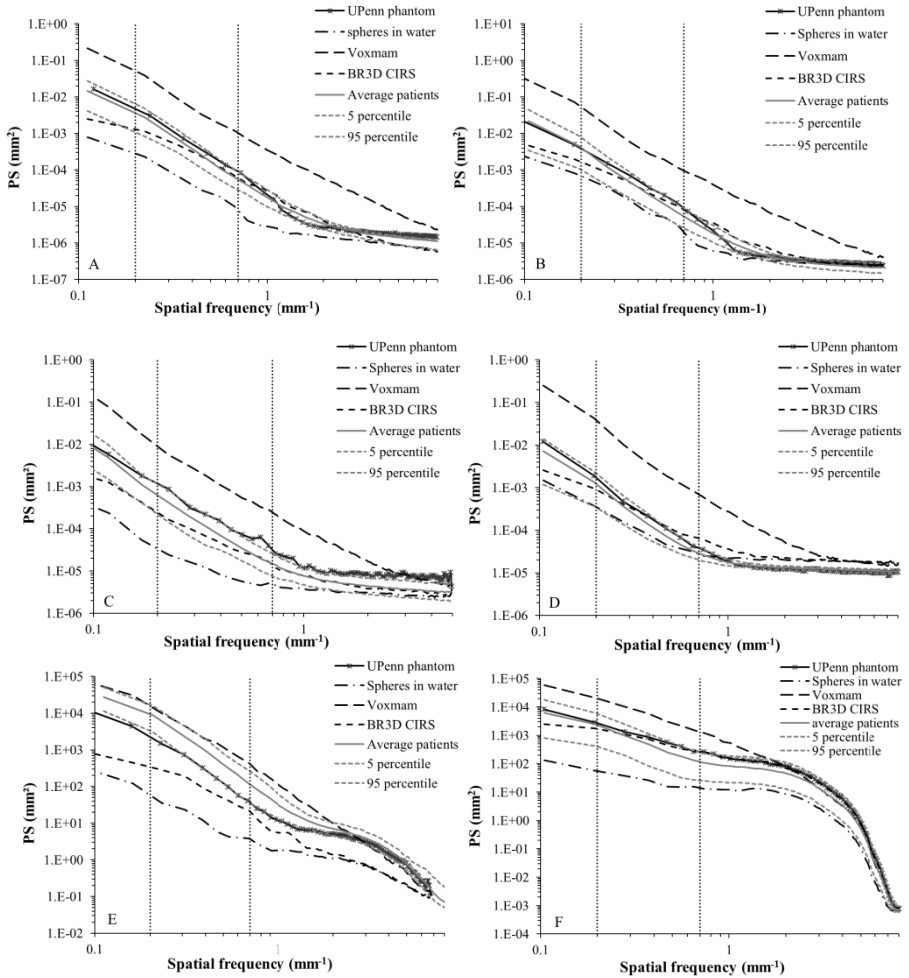


Fig. 3. Power spectrum curves of the UPenn phantom compared to three other structured phantoms and patients for the Hologic system (left) and the Siemens system (right) for 2D images (A) and (B), central DBT projections (C) and (D), and central reconstructed planes (E) and (F).

Finally, the mean glandular dose (MGD) was calculated for the UPenn phantom exposures under AEC for 2D and DBT, and the values were plotted against previously assessed patient doses [3]. For Hologic, the MGD is 1.21 mGy and 1.38 mGy while

for Siemens, it is 0.74 mGy and 1.70 mGy for 2D and DBT respectively. The phantom doses are within the patient dose range and below the achievable dose level set up for 2D mammography. However, 2D and DBT phantom doses fall within the lower segment of the patient dose range for Siemens. For Hologic, only a small difference in dose for 2D and DBT phantom exposures is found.

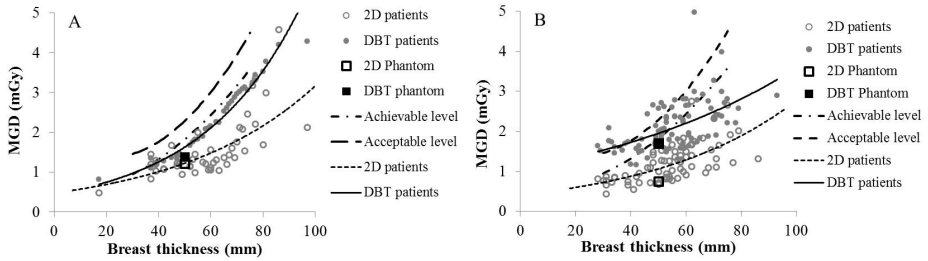


Fig. 4. Mean glandular doses for 2D and DBT phantom and patient images for Hologic (A) and Siemens (B)

A limitation of this study is that only a limited amount of patient data are included in our patient dataset. The launch of a general phantom validation procedure should start from a database that is representative for a general screening population. Finally, given the large technical differences between DBT systems, a general conclusion is only possible after tests on other DBT systems are completed.

4 Conclusions

In conclusion, this study tested the anthropomorphic structure of the newly designed UPenn phantom against patient breast structure for 2D and DBT imaging in terms of power spectra and power law coefficients. The phantom structure was found to be a good candidate for DBT performance testing with dose properties similar to patient doses. In future, simulated lesions or lesion-like objects will be inserted in the phantom, allowing clinically relevant detection tasks.

References

1. Pokrajac, D.D., Maidment, A.D.A., Bakic, P.R.: Optimized generation of high resolution breast anthropomorphic software phantoms. *Med. Phys.* 39(4), 2290–2302 (2012)
2. Brunner, C.C., Acciavatti, R.J., Bakic, P.R., Maidment, A.D.A., Williams, M.B., Kaczmarek, R., Chakrabarti, K.: Evaluation of various mammography phantoms for image quality assessment in digital breast tomosynthesis. In: Maidment, A.D.A., Bakic, P.R., Gavenonis, S. (eds.) *IWDM 2012. LNCS*, vol. 7361, pp. 284–291. Springer, Heidelberg (2012)
3. Cockmartin, L., Bosmans, H., Marshall, N.W.: Comparative power law analysis of structured breast phantom and patient images in digital mammography and breast tomosynthesis. *Med. Phys.* 40(8), 0189201–01892017 (2013)